Coupled adsorption/precipitation (Γ/Π) modelling of scale inhibitor transport in porous media using the coupled isotherm, $A_{\Gamma\Pi(}$**c)**

Colloids and Surfaces A: Physicochemical and Engineering Aspects 703 (2024) 135309

Contents lists available at ScienceDirect

Colloids and Surfaces A: Physicochemical and Engineering Aspects

journal homepage: www.elsevier.com/locate/colsurfa

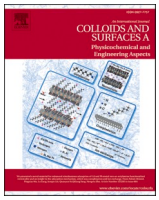

Coupled adsorption/precipitation (Γ/Π) modelling of scale inhibitor transport in porous media using the coupled isotherm, $A_{\Gamma\Pi}(c)$

M. Kalantari Meybodi *, K.S. Sorbie, O. Vazquez, E.J. Mackay

Institute of GeoEnergy Engineering (IGE), Heriot-Watt University, Edinburgh, UK

HIGHLIGHTS

- Transport model coupled with adsorption/ precipitation (Γ/Π) isotherm to simulate coupled squeeze treatment.
- Higher concentration region in return profile is controlled by Π and dissolution kinetics.
- Lower concentration region is controlled by Γ.
- Middle concentration is controlled by both Γ and Π.
- Π can extend the lifetime of squeeze treatments by some folds especially for treatments with higher MIC.

GRAPHICAL ABSTRACT

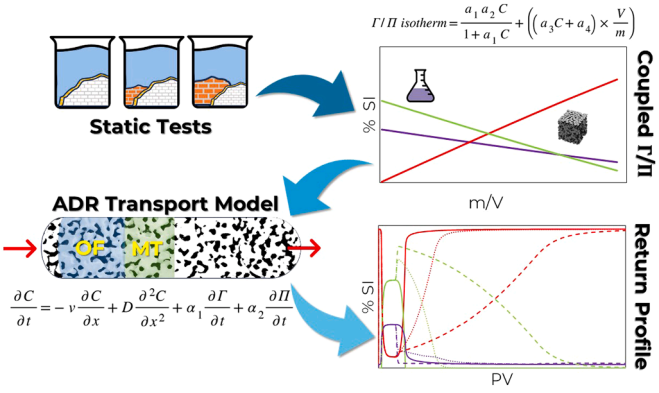

ARTICLE INFO

Keywords:
Coupled squeeze modelling
Reactive transport
Precipitation
Adsorption
Coupled ΓΠ isotherm
Scale inhibitor

ABSTRACT

Scale inhibitor (SI) "squeeze" treatments are widely used operations in production assurance to prevent inorganic scales as one of the main flow assurance problems. In these treatments, a high concentration SI slug is injected ("squeezed") into the porous medium, retained in the formation rock, and is gradually produced back at relatively small concentrations that can prevent (or significantly reduce) scale formation. The retention of SI in the formation is governed by coupled mechanisms of adsorption (Γ) and precipitation (Π) of SI species in the system. To design such SI treatments in an optimized manner, it is important to have good mathematical models of both the transport and the coupled interactions of adsorption/precipitation (Γ/Π) processes. In this study, a 1D advection-dispersion-reaction transport model has been developed, considering the coupled Γ/Π retention processes, and it is used to model linear core flood systems. The parameters for the equilibrium Γ/Π model can be derived from the routine bulk SI "apparent adsorption" tests that are usually conducted before any treatments. From previous works, equilibrium adsorption isotherm, Γ(c), is used to describe the adsorption behavior in such systems. However, although the precipitation kinetics are "fast" (almost at equilibrium), the kinetics of SI dissolution are "slow" and is therefore modelled by a kinetic rate law. From the derived dimensionless form of the transport-Γ/Π model equations, it is shown that the system is governed by 4 dimensionless numbers, N_A, N_P, N_{Pe} and N_{Da}, which are the adsorption number, the precipitation number, the Peclet number, and the Damköhler number, respectively. The shape of the adsorption isotherm also plays a very important part in the extent and

* Corresponding author.
E-mail addresses: mk2039@hw.ac.uk, mahdikalantari@gmail.com (M. Kalantari Meybodi).

https://doi.org/10.1016/j.colsurfa.2024.135309
Received 2 August 2024; Received in revised form 28 August 2024; Accepted 6 September 2024
Available online 12 September 2024

form of the effluent SI returns from the linear system. The developed model was then employed to carry out a series of sensitivity calculations relating to coupled adsorption/precipitation (Γ/Π) processes. Both equilibrium and kinetic SI precipitation were modelled coupled with the equilibrium SI adsorption, and the effect of these processes on the form and extent of the SI effluents was assessed. A range of sensitivities was then carried out to determine the effect of a wide range of parameters, including the effects of flow rate and shut-in periods on the kinetic dissolution effluent behavior. The findings from this work present the most clear explanation to date of why and how "precipitation squeezes" can greatly extend squeeze lifetime. A novel feature of this analysis is to show how the role of precipitation and adsorption changes over the various stages of the return effluent by developing plots of the %SI adsorbed on the rock, in the precipitate, and the mobile fluid phase.

1. Introduction

Inorganic scale formation is one of the largest problems in the energy industry, and it can be very expensive to prevent or remediate. Scales, such as barium sulfate, calcium carbonate, or magnesium silicate, can occur in different locations in production and injection streams, such as in pipelines, heat exchangers, wells, and in some cases within the porous medium itself. This usually occurs in situations where two incompatible brine streams comingled or there is a change in system's thermodynamical conditions like pressure and temperature, causing changes in the solubility of the inorganic salts that are present [1]. Since the removal of pre-deposited inorganic scales is usually very expensive, then the application of prevention and inhibition procedures is usually more favorable [2]. One of the most widely applied scale prevention methods is by applying phosphonate or polymeric scale inhibitors (SI) which are usually very effective and can be used in most cases at the point of mineral scale formation [3–5].

Scale inhibitors (SI) are chemicals that inhibit or reduce the rate of formation of inorganic scales [5,6]. One of the most important groups of SIs is the phosphonate scale inhibitors, such as diethylenetriamine penta methylene phosphonic acid (DETPMP). The phosphonates, like all SIs, are weak poly acids (of the form H_nA) that can be dissociated, and in the dissociated form, their negatively charged species can form strong complexes with divalent ions, such as Ca^{2+} and Mg^{2+} [2,7–9]. Some of this resulting SI/Ca/Mg complex can remain in the solution and inhibit the formation of mineral scales, but some of the complex precipitates, especially at higher SI concentrations. Different phosphonate SIs have different capacities for forming complexes with a maximum coordination number of divalent ions equal to the number of phosphonate groups; i.e. 5 for DETPMP, 6 for OMTHP, 4 for HMDP, etc. [2,7–10]. The precise *average* stoichiometry of the equilibrium SI/Ca/Mg complex is denoted SI_Ca_{N1}_Mg_{N2} in the previous publication from this group [11], where N_1 and N_2 are molar ratio of Ca and Mg to SI respectively.

When SIs are applied downhole in a producing (oil or geothermal) well, they are usually applied in a "squeeze treatment" [3–5,12]. This process involves injecting a slug of high-concentration SI (e.g. ~100, 000 mg/L) into the formation followed by an over flush to displace it further into the porous media to invade and contact a larger volume of the rock formation. A shut-in (no flow) period of the well then allows the injected SI to react and reach the equilibrium with the rock and *in situ* formation fluid, when the coupled processes of adsorption (Γ) and precipitation (Π) may occur at this stage. Finally, the back production of the well re-commences when the SI may desorb from the rock or the formed precipitate may dissolve back into the flowing stream, and this SI in the produced brine is available to prevent or reduce the mineral scale formation. Typically, in the back production period, the SI effluent concentration returns show a high concentration peak which is comparable to the injected concentration of the SI. This is followed by a decreasing concentration "tail" which, in a well-designed treatment, will give a very extended period of "time" (or volume of brine produced) at a concentration above the Minimum Inhibitor Concentration (MIC), which is the threshold SI concentration capable of preventing or significantly reducing the amount of inorganic scale formation [3,13,14]. To be effective, the SI MIC should be well below the amount of scale in molar terms i.e. it should be significantly sub-stoichiometric in terms of moles of scale prevented [3,14,15]. This MIC can be as low as 1 mg/L to ~ 10 s to 100 s of mg/L of active SI. When the SI concentration drops below MIC, a new squeeze treatment must be implemented. The time period taken for the return SI concentration drops below MIC after commencing a squeeze treatment, is known as the squeeze lifetime [16–18]. In this context "lifetime" in the field may be measured in a volume of produced brine treated by SI at a concentration >MIC, and in the lab, this may be the volume in core pore volumes (PV) that it takes for the effluent SI concentration to drop below the MIC. Considering the operation cost and efficiency, it is generally more desirable to have an extended squeeze lifetime for each squeeze treatment. It has been shown that efficiently designed squeeze treatments can save many millions of dollars each year in a single field for operating companies [14,16,19].

The squeeze lifetime depends strongly on the SI retention mechanisms that operate in the porous medium [20,21]. It is well known that two main mechanisms control SI retention in a given porous medium (rock or sand) system. The first mechanism is SI **adsorption** (Γ), which is described by an adsorption isotherm, Γ(C), in which, charged dissociated SI molecules, are adsorbed on the rock surfaces and these may subsequently desorb back into the flowing fluid as the SI concentration decreases in the bulk aqueous phase [22–25]. Adsorption occurs in virtually *all* cases and in some systems, such as sandstones, it is usually the sole governing mechanism that determines the squeeze lifetime [26]. The second mechanism is SI **precipitation** (Π), in which the charged SI molecules, create complexes with Ca^{2+} and Mg^{2+} which are sparingly soluble and hence may precipitate in the system. These precipitates can later redissolve slowly into the bulk flowing fluid as the SI concentration decreases in the system [11,24,25,27–31]. This mechanism usually occurs in the systems where a high concentration of Ca^{2+} and Mg^{2+} exist in the formation water or in reactive formations that have these cations in their mineralogy and can release these divalent cations by changing system conditions (e.g. pH). This usually occurs in carbonate reservoirs such as calcite ($CaCO_3$) and dolomite ($CaMg(CO_3)_2$) formations [11].

SI squeeze treatments in which both adsorption and precipitation occur together are often called "precipitation squeezes" and it is thought that the role of precipitation is more important in determining the squeeze lifetime in such treatments [11,22,29,32]. In this study, it is shown that the interaction between the coupled adsorption and precipitation processes is a little more complex and the 2 mechanisms actually work together to extend the squeeze lifetime.

Many researchers have studied adsorption squeeze treatments where the SI adsorption isotherm Γ(C), is usually modelled using one of the adsorption isotherm expressions in the literature, such as the Langmuir or Freundlich isotherm equations [30,33–37]. Others have investigated the coupled adsorption/precipitation squeeze treatments but most of them are usually developed for specific systems or require some parameters that are not usually available in the field application cases [28, 29,32,38–41].

In this paper, a transport model has been developed to model the coupled adsorption/precipitation (Γ/Π) squeeze treatment, in which the recent coupled Γ/Π isotherm [11] is used to express the joint interactions of adsorption and precipitation for the first time. The coupled

Γ/Π isotherm is derived from routine static "apparent adsorption" test results [24,32]; it may be used directly in the developed transport model to easily simulate coupled squeeze treatments, without the need for advanced parameters that might be required in other models. In this model, the system is presented *as if* the SI was a single component of concentration, c. In this study, only dissolution of the SI precipitate is considered to be kinetic, and adsorption is assumed to be at equilibrium. There may also be some small additional effect of kinetic adsorption and this is currently under investigation (Kalantari Meybodi *et al.*, in preparation). However, as noted in the literature review above, an SI in a carbonate core would be highly reactive, and indeed this would contribute to its precipitation (Π). In a previous study [11], authors have presented the full multicomponent coupled equilibrium model for the SI (phosphonate)/ calcium carbonate / SI_Ca-Mg complexation system and matched this with static "apparent adsorption" experiments [11]. This full equilibrium coupled system involved up to 3 n+14 components (where n is the protonation capability of SI, e.g: n=10 for DETPMP which resulted in 44 components) and it also included adsorption and precipitation using the Γ/Π model (see below) [2,11]. The final version of our transport code will include this full multicomponent model, with all the many species involved. However, given the complexity of the results, we are first presenting this simpler model (single SI species model, kinetic precipitation dissolution) in order to baseline for the fundamental sensitivities that can be seen in this simpler (but far from trivial) system and the template for the methodology of the implementation of recent Γ/Π model [11] in the transport model. Broadly similar results are found in the fully coupled system, but there are also several additional effects that will be described in a forthcoming paper for some specific systems (Kalantari Meybodi *et al.*, in preparation). Also, the tunning procedure of the fully coupled system has been developed and will be presented in that paper (Kalantari Meybodi et al., in preparation).

2. Model development for coupled Γ/Π squeeze treatment system

2.1. Governing transport – Γ/Π equations

The generalized **dimensional** equation for fluid transport through a porous medium including adsorption (Γ) and precipitation/ dissolution (Π) can be expressed as follows (where the various terms and units are given):

$$\left(\frac{\partial c}{\partial t}\right) = -v\left(\frac{\partial c}{\partial x}\right) + D\left(\frac{\partial^2 c}{\partial x^2}\right) - \alpha_1\left(\frac{\partial \Gamma}{\partial t}\right) - \alpha_2\left(\frac{\partial \Pi}{\partial t}\right)$$

$$c = SI\ concentration,\ mg/L$$

$$v = fluid\ velocity,\ length/time - cm/s$$

$$D = diffusion/dispersion\ coefficient,\ length^2/time - cm^2/s$$

$$\Gamma = SI\ adsorption - described\ by\ an\ adsorption\ isotherm,\ mg/g \quad (1)$$

$$\Pi = SI\ precipitation - model\ in\ text,\ mg/g$$

$$\alpha_1\ and\ \alpha_2 = dimensional\ correction\ factors = \rho/\phi\ (i.e.\ here\ \alpha_1 = \alpha_2)$$

$$\rho\ and\ \phi = density\ (mass/length^3;\ g/L)\ and\ porosity,\ respectively$$

$$NB\ \left(\frac{\rho\Gamma}{\phi}\right)\&\left(\frac{\rho\Pi}{\phi}\right) = mg\Big/L\ (concentration\ units)\ if\ \rho\ is\ in\ g\Big/L$$

To model the transport and the adsorption/precipitation (Γ/Π) processes, then rate laws must be specified for both the adsorption and precipitation terms in Eq.1. Assuming that adsorption (Γ) is at equilibrium but precipitation/dissolution (Π) is kinetic, after some rearrangement, the following (still dimensional) equations can be obtained:

$$\left(1 + \alpha_1\left(\frac{\partial \Gamma}{\partial c}\right)\right)\left(\frac{\partial c}{\partial t}\right) = -v\left(\frac{\partial c}{\partial x}\right) + D\left(\frac{\partial^2 c}{\partial x^2}\right) - \alpha_2\left(\frac{\partial \Pi}{\partial t}\right) \quad (2)$$

The kinetic precipitation/dissolution rate law must also be defined, which it is assumed to be of the following form here:

$$\left(\frac{\partial \Pi}{\partial t}\right) = \kappa\left(\Pi_{eq}(c) - \Pi\right)$$

$$\kappa = dissolution\ rate\ constant\ (1/time;\ 1/s) \quad (3)$$

$$\Pi_{eq}(c) = equilibrium\ precipitation\ at\ SI\ concentration,\ c(mg/g)$$

The above equations can be cast in dimensionless form using following dimensionless variables:

$$C = \frac{c}{c_0}; X = \frac{x}{L}; T = \frac{v}{L}t; \Gamma' = \frac{\Gamma}{\Gamma_{\max}}; \Pi' = \frac{\Pi}{\Pi_{\max}}$$

$$c_0 = \ maximum\ applied\ SI\ concentration\ (mg/L) \quad (4)$$

$$L = \ length\ of\ linear\ system\ or\ max\ radius\ of\ radial\ system\ (cm\ or\ m)$$

Combining Eq.2 to Eq.4 gives following governing equations in dimensionless variables:

$$\left(1 + N_A\left(\frac{\partial \Gamma'}{\partial C}\right)\right)\left(\frac{\partial C}{\partial T}\right) = -\left(\frac{\partial C}{\partial X}\right) + \left(\frac{1}{N_{Pe}}\right)\left(\frac{\partial^2 C}{\partial X^2}\right) - N_P.N_{Da}\left(\Pi'_{eq}(C) - \Pi'\right) \quad (5)$$

and

$$\left(\frac{\partial \Pi'}{\partial T}\right) = N_{Da}\left(\Pi'_{eq}(C) - \Pi'\right) \quad (6)$$

where the 4 dimensionless numbers above have the following form and meaning:

$$N_A = \left(\frac{\alpha_1 \Gamma}{c_0}\right)\ (Adsorption\ number) \quad (7)$$

$$N_P = \left(\frac{\alpha_2 \Pi}{c_0}\right)\ (Precipitation\ number) \quad (8)$$

$$N_{Pe} = \left(\frac{vL}{D}\right)\ (Peclet\ number) \quad (9)$$

$$N_{Da} = \left(\frac{\kappa L}{v}\right)\ (Damköhler\ number\ (dissolution)) \quad (10)$$

The numbers N_A and N_P, express the relative magnitudes of the levels of SI adsorption and precipitation, respectively, relative to the applied concentration of SI, c_0. The Peclet number describes the balance between advection and dispersion, which in this particular application, it is not of major importance since the system is quite advection-dominated with some small degree of dispersive mixing which does not significantly affect these processes. Also, the front is self-sharpening because of the shape of the adsorption isotherm, and the "tail" of the displacement is very spread out by the adsorption-related dominating rarefaction wave. Finally, the Damköhler number is the ratio of the fluid flow rate (residence time) to the time scale of the dissolution rate, as the precipitate dissolves back into the flowing stream, which can be rearranged as:

$$N_{Da} = \left(\frac{\kappa L}{v}\right) = \left(\frac{L/v}{1/\kappa}\right) = \left[\frac{System\ transit\ (residence)\ time}{Reaction\ time}\right] \quad (11)$$

The corresponding equations for a radial system have been developed and coded in our work since the SI will be applied in a near-well radial system in field applications [28,31,38]. However, these are not presented here since the main focus of this paper is to interpret and

model laboratory scale linear core floods, where L~ 30 – 50 cm.

The initial conditions (IC) and boundary conditions (BC1 at the inlet x= 0 and BC2 at the outlet, x = L) are specified as follows:

$$\begin{array}{rcl} & & \textit{Initial Conditions} \\ IC \Rightarrow c(x,0) = [SI] = 0, 0 < x \le L, \quad t = 0\ (all\ cells) & & \\ & & \textit{Boundary Conditions} \\ BC1\ at\ x = 0\ (cell\ 0) & \Rightarrow & c(0,t) = c_0 = [SI]_{inj}, \quad 0 < t \le t_{inj} \\ & \Rightarrow & c(0,t) = 0, \quad t > t_{inj} \\ BC2\ at\ x = L\ (cell\ n) & \Rightarrow & c(L,t) = [SI]_n, \quad t \ge 0 \end{array} \tag{12}$$

where t_{inj} is the injection time (in PV for dimensionless equations) and $[SI]_{inj}$ is the injected SI concentration, c_o (in mg/L or 1 in dimensionless units defined above). These equations can be solved numerically using routine finite difference numerical methods and the implicit Crank-Nicolson method was applied in this case; where numerical solutions were found to be stable and robust.

2.2. Form of the Γ/Π isotherm, $A_{\Gamma\Pi}(c)$

To determine the amount of adsorption (Γ) and precipitation (Π) that are occurring in a bulk experiment, a mass, m, of a reactive solid substrate (say $CaCO_3$) is added to a volume, V, of an aqueous solution of given SI initial concentration, c_0. The initial mass of SI, m_{SI0}, in this system is clearly $m_{SI0} = Vc_0$. When the system comes to an equilibrium, the final SI concentration in solution is denoted, c_{eq}; thus the mass of SI "missing" from the solution is, $m_{SIf} = Vc_0 - Vc_{eq}$. If only adsorption (Γ) occurred in this system (i.e. no precipitation; Π =0) then, obviously the adsorption level is given by, $\Gamma = V(c_0 - c_{eq})/m$, where using the units above it can be seen that Γ is in units of mg/g. Now assume in this experiment that *actually* ***both*** adsorption (Γ) and precipitation (Γ) occurred, but this would not be obvious by directly observing a normal bulk experiment in a beaker or sample bottle. However, the same quantity is calculated as above, *assuming* it is all adsorption (which it is not), then the "apparent adsorption" is obtained, $\Gamma_{app} = V(c_0 - c_{eq})/m$, and this is so-called since it is not really adsorption, it is actually the sum of the true adsorption and the true precipitation; i.e. $\Gamma_{app} = \Gamma + \Pi$. A great deal of work has been carried out at this laboratory on the apparent adsorption in several systems and its usefulness in characterizing the partitioning between the true Γ and Π components of this quantity [21,26,42]. These previous studies have clearly demonstrated that there are 2 regions, as follows, (i) a region of pure adsorption (Γ) at lower SI up to a threshold concentration, c_{th} (usually c_{th} ≈100 mg/L) where an adsorption isotherm, Γ(c), applies (i.e. $\Gamma_{app} = \Gamma$) and there is no dependence on the solid mass/liquid volume ratio, (m/V), and (ii) a region of coupled adsorption/precipitation (Γ/Π) for c > c_{th} where the apparent adsorption is a function of (m/V) as shown schematically in Fig. 1.

The problem with the direct use of the bulk experimental apparent adsorption, Γ_{app}, in the flow model is because the mass to volume ratio, (m/V), in the bottle test and porous media, are very different; In fact, (m/V) ~ 250 g/L for the bottle-test whereas it can be (m/V) ~ 4000 g/L for a high porosity porous medium. Indeed, (m/v) may even be higher for lower porosity porous media (see below). However, this matter is dealt with by using the concept of the coupled Γ/Π isotherm, as described recently [11], and shown in Fig. 1. In essence, the approach extracts the separate contributions of the adsorption isotherm, Γ(c), and the precipitation function, $A_\Pi(c)$ vs. c, each of which is independent of the (m/V) ratio. Thus, in the transport model, the *local* values of Γ and Π, can be calculated for any value of SI concentration, c, using the local grid block value of (m/V) ratio. A full explanation is presented in reference [30].

From the previous study [11], the precipitation function was found to be a linear function as Shown in Fig. 1 and the adsorption is considered to follow the Langmuir isotherm. The coupled Γ/Π isotherm, $A_{\Gamma\Pi}$, is a combination of these 2 functions as represented mathematically below, where the parameters are chosen to match the experimental bottle tests. The full derivation of the coupled Γ/Π isotherm, its validation against experimental results can be found in the recent paper [11].

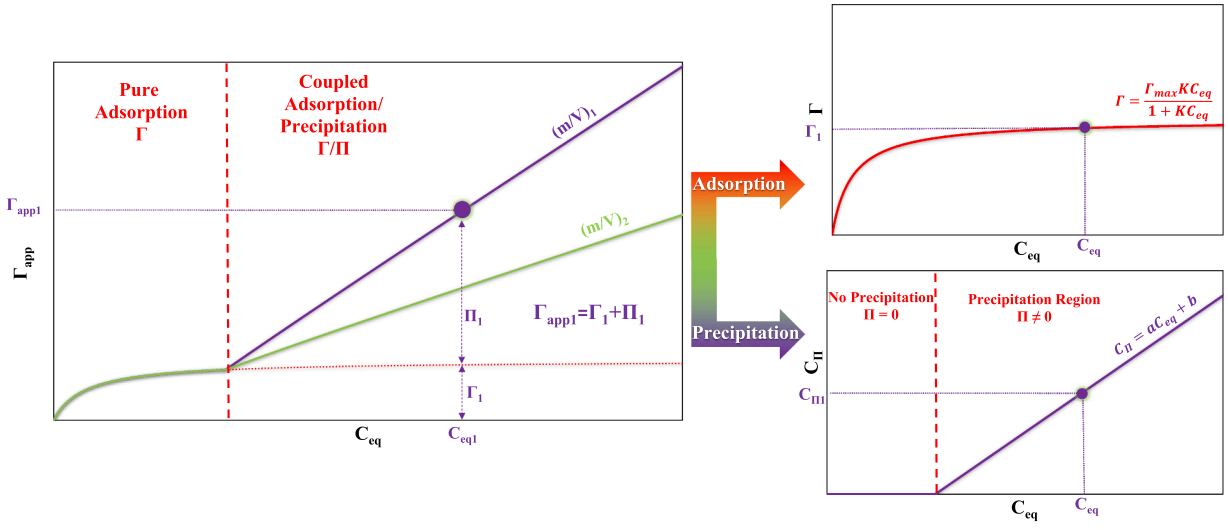

Fig. 1. Coupled adsorption/precipitation isotherm modelling [11].

Table 1
Effect of (m/V) ratio on the % distribution of SI in the coupled fluid/ Γ/Π system between the bulk solution, adsorption (Γ) and precipitation (Π).

Parameter	Unit	Bottle test	Porous media (core plug)
Porosity, ϕ	%	Powdered calcite	40
Mass of solid	g	10	226
Fluid volume	L	0.04	0.058
m/V	g/L	250	~3900
c_i	mg/L	1000	1000
Solution	% of c_i	38.29	24.33
Adsorption	% of c_i	3.19	47.02
Precipitation	% of c_i	58.52	28.65

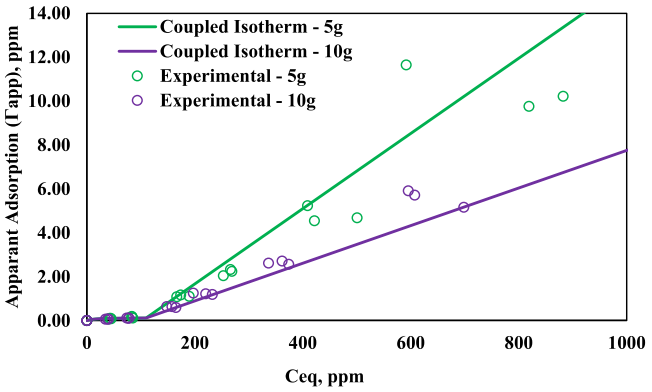

Fig. 2. Derived coupled adsorption/precipitation isotherm for a particular DETPMP-Calcite bulk "apparent adsorption" experimental system [11].

$$Coupled\ Isotherm,\ A_{\Gamma\Pi}(c) = \begin{cases} \dfrac{a_1 a_2 . c}{(1 + a_1 c)} \ for\ c \le c_{th} \\ \dfrac{a_1 a_2 . c}{(1 + a_1 c)} + (a_3 c + a_4)\left(\dfrac{V}{m}\right) for\ c > c_{th} \end{cases} \tag{13}$$

In Eq.13, Langmuir parameters a_1 and a_2 in Γ(c) correspond to $a_1 = K$ and $a_2 = \Gamma_{max}$, the maximum adsorption level, and the a_3 and a_4, correspond to the parameters in $c_\pi = a_3.c + a_4$, are the parameters in the Π(c) model, where $\Pi(c) = c_\pi$ (V/m).

The effect of the m/V ratio is shown for a typical bottle test and a very high porosity porous medium in Table 1. In this case, the tuning parameters of the coupled isotherm are assumed to be a_1=0.0773, a_2=0.1321 mg/g, a_3=2.1399, and a_4=-234.1626 mg/L as calculated previously based on the experimental values [11]. The match of this model to one of our bulk beaker apparent adsorption experiments is shown in Fig. 2, where the solid lines are the model (with the above parameters) and the points are experimental results [11,21,26]. As shown in Fig. 2 and in Table 1, the (m/V) ratio is used to directly scale the bottle test results to the porous medium, and it is shown that this significantly changes the distribution of the SI between adsorption, precipitation, and bulk fluid states. Specifically, the results in Table 2 show that in the porous medium, a much larger proportion of the SI is adsorbed (Γ), whereas in the bulk it is mainly in the precipitate (Π) form. This % distribution is shown as a function of (m/V) ratio in Fig. 3 and the "locations" of a bulk experiment and a porous medium are shown in this figure. As the (m/V) ratio increases, the mass of the solid that can adsorb the SI increases, and this causes the fraction of adsorbed SI to increase while the fraction of SI that is precipitated and that which remains in solution both decrease.

The distribution of SI between adsorption, precipitation, and solution, also depends on the initial SI concentration, as shown in Fig. 3. We use the matched parameters for the coupled isotherm, $A_{\Gamma\Pi}(c)$, as described above with threshold concentration, $c_{th} \approx 109$ mg/L; i.e. up to c = 109 mg/L only pure adsorption occurs (see Fig. 3 - a for the 100 mg/L case). For the high concentration of 10,000 mg/L, the adsorption rapidly builds up to its maximum adsorption (a_2) and the precipitation rapidly builds up in the system and a high fraction of the SI occurs in the precipitated form.

Table 2
Model specifications.

Parameter	Value	Unit	Note
Core length, L	20	cm	
Diameter, D	0.75	cm	
PV(pore volume)	14.5	cm^3	$= \pi.L(D/2)^2\phi$
V_t (total core volume)	35.36	cm^3	$= \pi.L(D/2)^2$
Matrix	Calcite ($CaCO_3$)	-	
Matrix density, ρ	2.71	g/cm^3	
Porosity, ϕ	0.41	-	
Adsorption model	Langmuir	-	
Adsorption model a_1	0.0773	1/(mg/L)	$a_1 = K$
Adsorption model a_2	0.1321	mg/g	$a_2 = \Gamma_{max}$
Precipitation model	Coupled Isotherm	-	
Precipitation model a_3	2.1399	-	
Precipitation model a_4	−234.1626	mg/L	
c_i-SI	2000	mg/L	ppm(aqueous)
c_i-Tracer	2000	mg/L	ppm(aqueous)
Vol. flow rate, q*	0.1332	cm^3/min	
Injection time**	1000 (~9.2 PV)	min	
Overflush time**	19000 (~174.5 PV)	min	

* Flow rate, q, subject to change for sensitivity cases; base case q gives residence time in the core of 108.86 mins (1.81 h);
** subject to change based on the change in flow rate in different cases.

2.3. Coupling of coupled Γ/Π isotherm with transport model

The transport model now developed incorporating the coupled Γ/Π isotherm. To couple the transport model with the coupled Γ/Π isotherm, it is implemented in each timestep-grid block. The transport is first conducted for the timestep and the c_i^t is determined for each grid block. Then the coupled isotherm is used to determine the concentration of solution, adsorption, and precipitation SI considering all the SI concentrations to be back in the solution including c_i^t, c_Γ^{t-1}, and c_Π^{t-1}. Then, the c_Γ^t and c_Π^t are compared with c_Γ^{t-1} and c_Π^{t-1} to check if more precipitation/adsorption needs to be removed from the solution OR if some of the adsorbed/precipitated SI should be released back into the solution. Finally, the c_i^t, c_Γ^t and c_Π^t are updated for each grid block and the process proceeds to the next timestep.

2.4. Precipitation dissolution kinetics

It is accepted that adsorption and precipitation processes are usually fast and near equilibrium but, the dissolution of precipitates is thermodynamically slow. To account for this, the following kinetic equation is considered where κ is the kinetic rate constant.

$$c = c_{eq}(1 - e^{-\kappa t}) \tag{14}$$

To couple the kinetic with the transport model, after conducting the transport calculation in each timestep followed by the coupled adsorption/precipitation, if the $c_\Pi^t < c_\Pi^{t-1}$, the precipitation dissolution is triggered. In this case, the c_Π^t and c_{eq}^t will be updated as follows:

$$\Delta c_\pi^t = \left(c_\pi^{t-1} - c_{\pi,eq}^t\right)(1 - e^{-\kappa t}) \tag{15}$$

$$c_\pi^t = c_{\pi,eq}^t + \Delta c_\pi^t \tag{16}$$

$$c^t = c_{eq}^t - \Delta c_\pi^t \tag{17}$$

It means that the kinetics just let the dissolution occur only proportional to the timestep related to the equilibrium time of the dissolution and changes the precipitation and the solution support from the

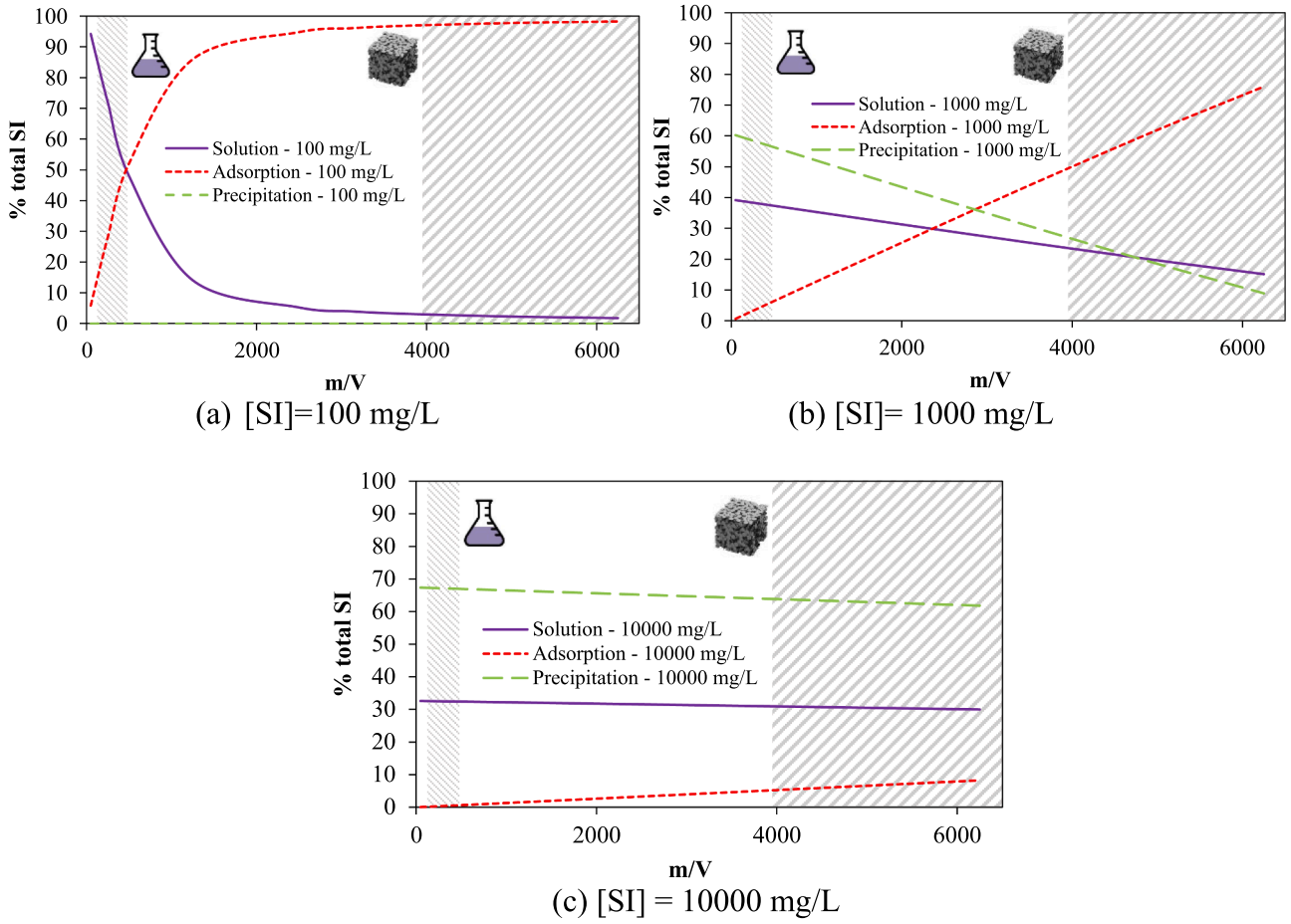

Fig. 3. Adsorption, precipitation, and solution distribution of SI vs. m/V ratio, based on the coupled Γ/Π isotherm for widely varying SI concentrations: (a) c_i=100 mg/L, (b) c_i=1000 mg/L, (c) c_i=10000 mg/L; the graphics show the typical ranges of (m/V) ratios (shaded) for the bulk solution laboratory measurements (i.e. in apparent adsorption experiments) [flask] and in porous media [rock].

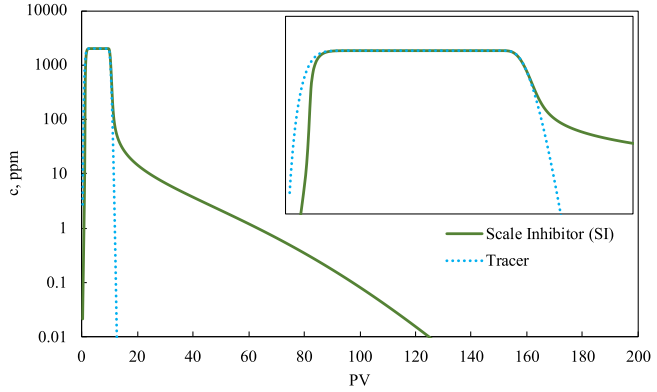

Fig. 4. Return profiles of the pure adsorption system, Case 1.

precipitation based on it.

3. Results and discussion

As discussed in the methodology section, the coupled isotherm is the heart of the developed transport model in this study. Here, the coupled isotherm that has been developed previously based on the experimental data is used [11].

3.1. Model specifications

To apply the transport model, a discretized linear model is considered with the specifications in Table 2.

3.2. Case 1: pure adsorption

The first calculation presented is the pure adsorption case, which is the baseline for later cases including precipitation (equilibrium and kinetic). Adsorption is described by the Langmuir model in this study with

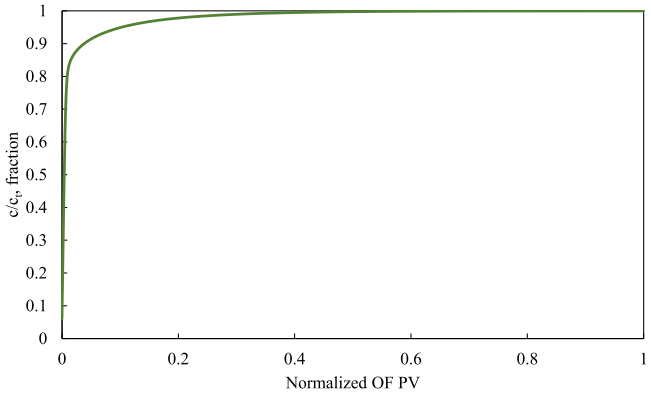

Fig. 5. Produced total SI in the system vs. normalized production volume for a pure Γ system.

parameters of a_1 and a_2 (Table 2). Fig. 4 shows the effluent profiles for this case for the SI and tracer. Clearly, the SI breakthrough occurs later than the tracer due to SI adsorption in the system. Also, because of the form of the adsorption isotherm, a long tail is observed for the SI which is shown that after more than 60 PV of over flush, the SI concentration is still $>$ 1 mg/L. This illustrates the main idea of using an adsorption squeeze treatment to maintain an appropriate level of SI (higher than MIC) for a long time after a very limited injection of SI. This process has been studied for many years and is well explained in the literature [23, 28–31,34].

It is well known that in an adsorption squeeze, then very soon after the overflush (OF) commences, the majority of the SI is produced back, as shown in Fig. 5. In this case, more than 95 % of the SI in this system, has been produced back in 0.2 of normalized OF PV (~35 PV). This back-produced SI does not contribute to later scale prevention and is a serious loss of effective chemicals. Precipitation squeeze treatments have been studied extensively in recent years in order to remedy this early loss of SI. It may be thought that this issue could be tackled by increasing the SI adsorption (increasing Γ_{max}). This does help to extend squeeze lifetime, but due to the nature of SI and rock substrates, the maximum adsorption possible is quite limited. However, this benefit may be reduced or lost if Γ_{max} is too high since the SI cannot be propagated sufficiently deep into the near well formation.

3.3. Case 2: equilibrium coupled adsorption/precipitation (Γ/Π)

We now consider Case 2 where ***equilibrium*** coupled adsorption/precipitation (Γ/Π) takes place; i.e. *both* adsorption (Γ) and precipitation (Π) are locally at equilibrium. Fig. 6 shows a comparison of this equilibrium Γ/Π case (Case 2) with the adsorption-only case (Case 1). The full SI return curves are shown in Fig. 6 and the early-time effluent profiles are also shown inset in this figure. The most striking feature of this calculation is that, although extensive precipitation does occur (described by the Γ/Π model described above), it makes very little difference to the SI return curves in the long tail where the higher SI effect is required. It only makes a difference in the early time where the high concentration SI profile shows an initial delay of breakthrough due to precipitation, and during the overflush a "shoulder" appears due to rapid dissolution of the precipitate (see Fig. 6). This contributes little to scale inhibition in the longer tail, where it is most required. The precipitate function C_Π vs. [SI] indicates that the precipitate is in fact quite soluble and so it is simply redissolved very quickly into the flowing aqueous phase and is produced from the system.

3.4. Case 3: kinetic coupled adsorption/precipitation (Γ/Π)

Case 3 is the first base case of the kinetic Γ/Π model where the adsorption (as in all cases) is at equilibrium but the redissolution part of

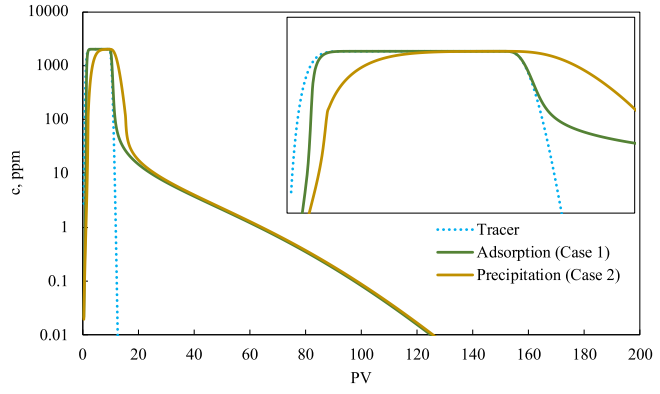

Fig. 6. Return profiles of an equilibrium coupled Γ/Π system (Case 2) compared with the adsorption only case (Case 1).

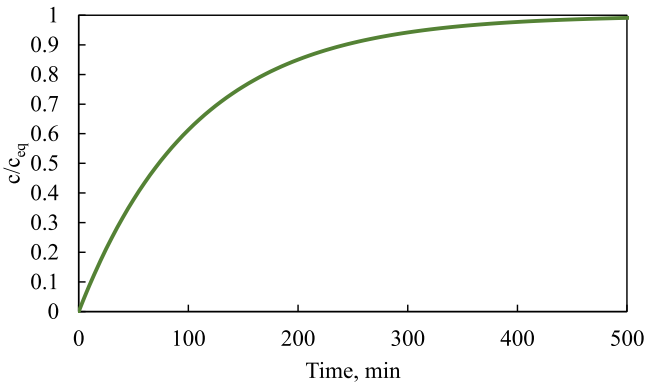

Fig. 7. Static precipitation dissolution kinetics, with of κ=0.0095 min^{-1}.

the precipitation process is kinetic. Literature data indicates that a DETPMP-Ca^{2+} precipitate takes ~ 8 h for the complex to redissolve into the aqueous phase at static conditions. Using this approximate value leads to a base case kinetic parameter (κ) of κ=0.0095 min^{-1}; and a static calculation using this value is shown in Fig. 7, from which it can be seen that by 8 h (480 mins) the c/c_0 value is ~0.97. Given that the base case flow rate is, q=0.1332 cm^3/min (Table 3), then the residence time of the SI in the core is ~108.86 min (1.81 h), it is expected to reveal kinetic effects since the ratio of reaction (dissolution) time/ residence time ~ (1.81/8) ≈ 0.23, which is only about a quarter of the time required to reach near equilibrium. This ratio is clearly related to ($1/N_{Da}$), the inverse of the Damköhler number.

The SI effluent profiles for Case 3, with dissolution kinetic parameter, κ=0.0095 min^{-1}, are shown in Fig. 8, where they are compared with Case 2 (equilibrium adsorption/precipitation) and Case 1 (pure adsorption). Note that the frontal part of the SI profile for both precipitation cases is the same (since they are at equilibrium – i.e. fast precipitation). The clear differences between these 2 cases appear in the long SI effluent tail where the kinetic precipitation (actually kinetic dissolution) case remains well above the equilibrium case for the entire return period, and the squeeze lifetime is extended, although this extension is modest in this case. However, this shows that the precipitation process can in principle extend the squeeze lifetime, but now example sensitivities are given to determine the key factors that may extend this lifetime even further.

3.5. Case 4: investigation of kinetic effects

The first sensitivity that is investigated is the kinetic dissolution rate constant (κ), although this variable must be considered in light of the flow rate (ν) at which the calculation is performed. This is evident from our analysis above from the dimensionless number governing the kinetics, the Damköhler number, $N_{Da} = (\kappa L/\nu)$. Thus, if we double the dissolution rate constant (κ) and double the flow rate (ν), the calculations are identical (we have confirmed this numerically). Therefore, we can first fix the dissolution rate constant and vary the flow rate to study this effect, although we return to this issue later in the paper.

Case 4–1: Effect of Flowrate

In this case, 3 flow rates are considered with the same kinetic parameter as Case 3 above (κ=0.0095 min^{-1}). The flow rates are q = 0.0666, 0.1332 (base case; Case 3), and 0.2664 cm^3/min for Cases 4.1.1, 4.1.2, and 4.1.3, respectively, in Table 3. Fig. 9 shows three quantities in the last grid cell of the model as follows: Fig. 9*(a)* the adsorbed amount of SI (as equivalent concentration), Fig. 9*(b)* the mobile phase SI concentration [this is effectively the effluent value observed in an experiment], and Fig. 9*(c)* the amount of SI precipitate (again as equivalent SI concentration).

Considering first the SI effluent results in Fig. 9*(b)*, it is evident that the flow rate (or kinetic parameter) has a significant effect on the SI

Table 3
Dimensionless groups for all cases.

	Case	Title	Case No.	Specification	N_A	N_P	N_{Da}
	1	Pure Adsorption	1		0.4475	0	-
	2	Equilibrium Coupled Adsorption/ Precipitation (Γ/Π)	2		0.4475	3.5128	∞
	3	Kinetic Coupled Adsorption/ Precipitation (Γ/Π)	3	κ =0.0095 min^{-1}, q_{OF}=0.1332 cm^3/min for all cases unless otherwise stated.	0.4475	3.5128	2.5219
Kinetic Effects Investigation	4.1	Effect of Flowrate	4.1.1	κ =0.0095 min^{-1}, q_{OF}=0.0666 cm^3/min	0.4475	3.5128	5.0438
			4.1.2	κ =0.0095 min^{-1}, q_{OF}=0.1332 cm^3/min	0.4475	3.5128	2.5219
			4.1.3	κ =0.0095 min^{-1}, q_{OF}=0.2664 cm^3/min	0.4475	3.5128	1.2610
	4.2	Shut-in Effect (q_{OF}=0.1332 cm^3/min)	4.2.1	κ =0.0095 min^{-1} shut-in= 1 h	0.4475	3.5128	2.5219
			4.2.2	κ =0.0095 min^{-1} shut-in= 12 h	0.4475	3.5128	2.5219
			4.2.3	κ =0.0095 min^{-1} shut-in= 24 h	0.4475	3.5128	2.5219
Coupled Γ/Π Model Sensitivity Analysis	5.1	Effect of Kinetic Parameter (κ) (q_{OF}=0.1332 cm^3/min)	5.1.1	κ =0.001 min^{-1}	0.4475	3.5128	0.2655
			5.1.2	κ =0.0025 min^{-1}	0.4475	3.5128	0.6637
			5.1.3	κ =0.005 min^{-1}	0.4475	3.5128	1.3273
			5.1.4	κ =0.0075 min^{-1}	0.4475	3.5128	1.9910
			5.1.5	κ =0.01 min^{-1}	0.4475	3.5128	2.6547
			5.1.6	κ =0.025 min^{-1}	0.4475	3.5128	6.6366
	5.2	Effect of Γ_{max} (q_{OF}=0.1332 cm^3/min)	5.2.1	Γ_{max} =0.05 mg/g, κ =0.0095 min^{-1}	0.1694	3.5128	2.5219
			5.2.2	Γ_{max} =0.1 mg/g, κ =0.0095 min^{-1}	0.3388	3.5128	2.5219
			5.2.3	Γ_{max} =0.5 mg/g, κ =0.0095 min^{-1}	1.6938	3.5128	2.5219
			5.2.4	Γ_{max} =1 mg/g, κ =0.0095 min^{-1}	3.3875	3.5128	2.5219
			5.2.5	Γ_{max} =0.05 mg/g, Eq. precipitation	0.1694	3.5128	∞
			5.2.6	Γ_{max} =0.1 mg/g, Eq. precipitation	0.3388	3.5128	∞
			5.2.7	Γ_{max} =0.5 mg/g, Eq. precipitation	1.6938	3.5128	∞
			5.2.8	Γ_{max} =1 mg/g, Eq. precipitation	3.3875	3.5128	∞
			5.2.9	Γ_{max} =0.05 mg/g, No precipitation	0.1694	0	-
			5.2.10	Γ_{max} =0.1 mg/g, No precipitation	0.3388	0	-
			5.2.11	Γ_{max} =0.5 mg/g, No precipitation	1.6938	0	-
			5.2.12	Γ_{max} =1 mg/g, No precipitation	3.3875	0	-
	5.3	Coupled κ / Γ_{max} Sensitivity (q_{OF}=0.1332 cm^3/min)	5.3.1	Γ_{max}=0.05 mg/g, κ =0.001 min^{-1}	0.1694	3.5128	0.2655
			5.3.2	Γ_{max} =0.1 mg/g, κ =0.001 min^{-1}	0.3388	3.5128	0.2655
			5.3.3	Γ_{max} =0.5 mg/g, κ =0.001 min^{-1}	1.6938	3.5128	0.2655
			5.3.4	Γ_{max} =0.05 mg/g, κ =0.005 min^{-1}	0.1694	3.5128	1.3273
			5.3.5	Γ_{max} =0.1 mg/g, κ =0.005 min^{-1}	0.3388	3.5128	1.3273
			5.3.6	Γ_{max} =0.5 mg/g, κ =0.005 min^{-1}	1.6938	3.5128	1.3273
			5.3.7	Γ_{max} =0.05 mg/g, κ =0.01 min^{-1}	0.1694	3.5128	2.6547
			5.3.8	Γ_{max} =0.1 mg/g, κ =0.01 min^{-1}	0.3388	3.5128	2.6547
			5.3.9	Γ_{max} =0.5 mg/g, κ =0.01 min^{-1}	1.6938	3.5128	2.6547

Notes:
1. For all cases, q_{Inj} = 0.1332 cm^3/min, PV_{Inj} = 9.2, PV_{OF} = 174.5. q_{OF} = 0.1332 cm^3/min unless specified.
2. For all cases, N_{Pe}=40 which describes the dominant effect of the advective forces relative to the dispersive forces.

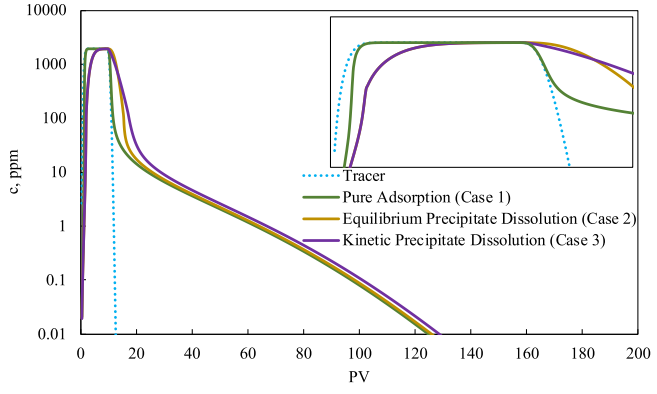

Fig. 8. Return profile of a coupled Γ/Π system considering kinetic precipitation dissolution (Case 3; kinetic dissolution of precipitate) along with a comparison with Case 2 (equilibrium adsorption and precipitation) and Case 1 (pure adsorption).

effluent profile, with a *higher flow rate* leading to a significantly improved SI return profile. This is equivalent to keeping a constant flow rate but making the kinetic dissolution rate constant (κ) *lower*. The corresponding results in Fig. 9*(a)* (adsorption, Γ, in the last grid block) and Fig. 9*(c)* (precipitation, Π) explain why the improved SI return curve is being seen in Fig. 9*(b)* at the higher flow rate. First examining the *low* flow rate cases in Fig. 9*(c)* shows that the kinetics quickly redissolves the SI complex to a higher concentration very early in the return period, and therefore there is very little precipitate left at a relatively early time (it is gone by ~10PV overflush); the corresponding result at the highest flow rate shows that there is more SI retained in the formation by precipitation – it is retained until about 30PV of overflush. The fundamental mechanism through which coupled adsorption/ precipitation improves the SI return curves in the long tail is due to the presence of the precipitation "feeding" the solution at elevated SI concentration and the corresponding (equilibrium) adsorption being at equilibrium at this higher SI concentration. As we noted, the presence of precipitate in the system even for the highest flow rate case is ~ 30PV, after which it is gone, and the system is then completely adsorption controlled.

Case 4–2: The Effect of Shut-in on the SI Effluent Profiles

Given that the dissolution of the SI-precipitate is kinetic, then this question arises that what would be the effect of a shut-in on the return profiles? It might intuitively appear that if a shut-in occurs after some time in the over-flush, then the kinetic dissolution proceeds, and the mobile phase SI concentration increases; then when the flow is resumed, there may be a benefit from this higher concentration of SI in the effluent. To study this effect, 3 simulations were performed of the base case (Case 3) but with shut-in periods of 1, 12, and 24 hrs; these are Cases 4.2.1, 4.2.2, and 4.2.3 in Table 3. The results are shown in Fig. 10 where it is evident that the shut-in has almost no effect, even though a small spike in SI concentration is observed in the SI return profiles just

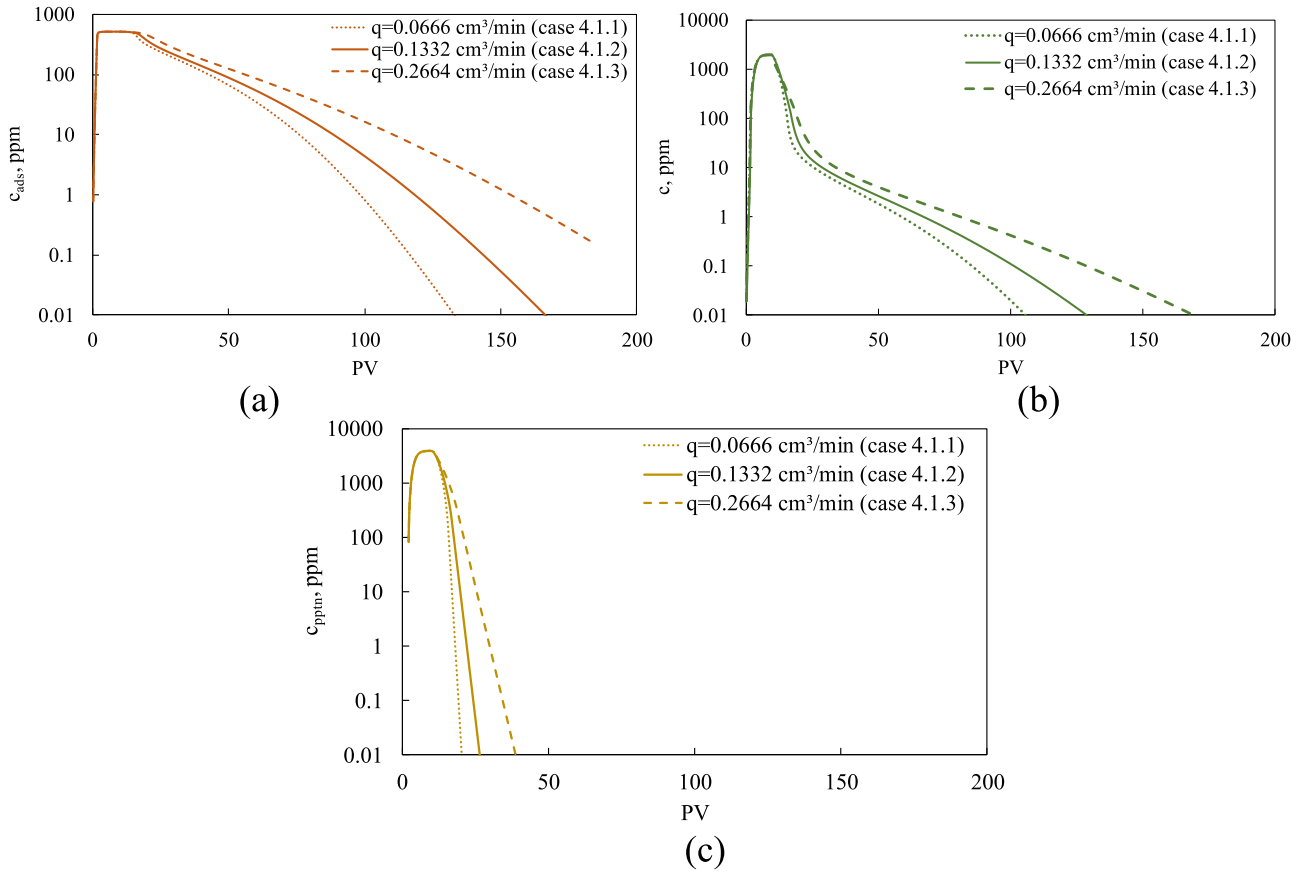

Fig. 9. Effect of flow rate on the kinetic coupled Γ/Π system concentration profiles (outlet cell): a) adsorption, b) solution, c) precipitation.

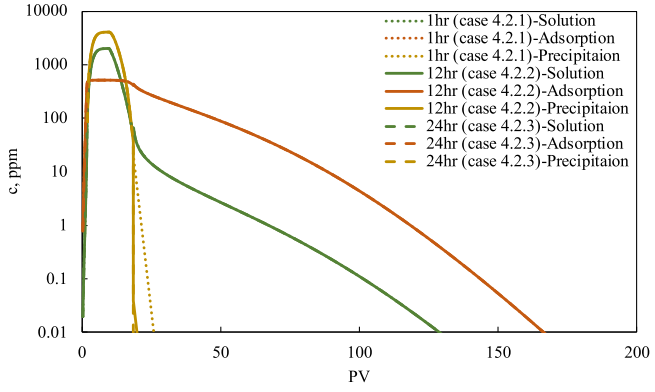

Fig. 10. Effect of shut-in on the kinetic coupled Γ/Π system concentration returns profiles (outlet cell).

after the shut-it. In fact, the reason for the lack of any significant effect is that the shut-in does redistribute the SI between the precipitate, adsorption, and the mobile phase, but the return curve is governed by the shape of the adsorption isotherm at that point and this moves the return curve very little, after ~1–3 PV following the shut-in the system is almost exactly where it was previously, apart from the amount of precipitate being a little less. Indeed, by material balance, the shut-in cases are very marginally worse than the case with no shut-in although this is almost imperceptible in the return curves in Fig. 10.

3.6. Case 5: coupled Γ/Π model parameter sensitivity analysis

As discussed previously, the efficiency of the coupled Γ/Π squeeze treatment is characterized by the squeeze lifetime, which in turn depends on various parameters that will be investigated in this section. Specifically, the effects of the kinetic parameter (κ) and the maximum adsorption level ($a_2 = \Gamma_{max}$) in the Langmuir adsorption isotherm is investigated. Finally, the result of various combinations of these 2 parameters (κ and Γ_{max}) is presented, which interact in an interesting manner.

Table 4
Approximate reaction time for different κ values, the corresponding Damköhler numbers and the Cases in Table 3.

κ	Approximate Reaction Time*	Case	Damköhler No.	Residence time/ Reaction time
0.001	65 hrs	Case 5.1.1	0.2655	0.028
0.0025	26 hrs	Case 5.1.2	0.6637	0.070
0.005	13 hrs	Case 5.1.3	1.3273	0.139
0.0075	8.5 hrs	Case 5.1.4	1.9910	0.213
0.01	6.5 hrs	Case 5.1.5**	2.6547	0.278
0.025	2.5 hrs	Case 5.1.6	6.6366	0.742

* Defined as the time to reach ~98 % of the equilibrium value ($c/c_{eq} \sim 0.98$)
** Very close to the base case (which has $\kappa = 0.0095\ min^{-1}$).

Case 5–1: Sensitivity to the Kinetic Parameter, κ

The calculations in Case 4.1 above showed clearly that kinetic consideration can have a significant effect on the squeeze lifetime, and its possible enhancement. The relation between the flow rate and the kinetic dissolution parameter (κ) was also pointed out since they are

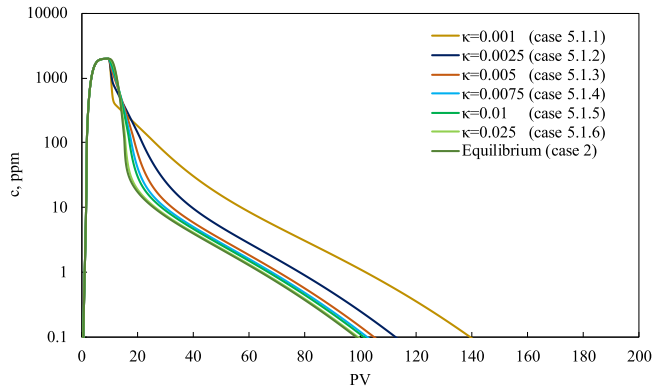

Fig. 11. Effect of κ on the return profile of the coupled Γ/Π system.

related through the Damköhler number ($N_{Da} = (\kappa L/v)$). A sensitivity analysis for the kinetic parameter is now presented, taking a wide range of κ values which are given, along with their corresponding Damköhler numbers in Table 3. The base case flow rate is maintained here (q = 0.1332 cm^3/min) giving a fluid (SI solution) residence time of ~1.81 h.

Using the κ values in Table 4 for the SI kinetic dissolution model gives the SI effluent return profiles presented in Fig. 11, where the kinetic cases (Cases 5.1.1 to 5.1.6 Table 3) are compared with the equilibrium return curve (Case 2; Table 3). As indicated above from our preliminary variable flow rate simulations (Cases 4.1.1 to 4.1.3; Table 3), the SI squeeze performance is strongly enhanced as the dissolution of the precipitated SI-complex becomes slower; i.e. at lower κ values. In addition, the results in Fig. 11 show that some more complex behaviour can occur at very low dissolution rates, where non-monotonic behavior is observed in the effluents.

To explain the effect of the dissolution rate (κ), we choose 2 of the cases from Fig. 11, with $\kappa = 0.001$ and 0.005 min^{-1}. Results for these 2 kinetic cases are compared with the equilibrium case in Fig. 12; where Fig. 12(a) shows the amount of adsorption (in equivalent concentration), Fig. 12(b) shows the mobile phase SI concentration (the usual SI return curve), and Fig. 12(c) shows the amount of precipitate (in equivalent concentration) in the last grid block of the core. In the slowest kinetic case ($\kappa = 0.001$ min^{-1}), it can be seen in Fig. 12(c) that the presence of precipitate persists for much longer (~100 PV of overflush) than in the higher dissolution rate case (~30 PV of overflush) and of course the equilibrium case, where it is very short-lived (~5 PV of overflush). The presence of the precipitate kinetically "feeds" the mobile phase with SI and correspondingly, the amount of precipitate reduces over time (Fig. 11(c)), over ~80PV this leads to a fairly level adsorption on the rock (Fig. 11(a)), and the adsorption isotherm retards the propagation of the SI causing a spread-out tail [38,41,43]. As the precipitate drops to a much lower level after 80PV, the SI "feed" from this source reduces and nearly stops and the remainder of the process is governed by the adsorption isotherm. This is the kinetic precipitation mechanism of the improvement in the SI return curve over a longer period.

A final confirmation of this mechanism is provided by the results in Fig. 13 which shows the *mass fraction* of the SI that is present in the system as adsorption, in the mobile phase, or as precipitate. Fig. 13(a) shows the equilibrium adsorption/precipitation case, Fig. 13(b) shows the case for $\kappa = 0.005$ min^{-1} and Fig. 13(c) shows the case for $\kappa = 0.001$ min^{-1}. These results essentially tell the same story as discussed above and they show that the balance between the precipitate contribution and the adsorption contribution to the SI return effluent increases and is more persistent over time (PV) at the lower kinetic dissolution rate.

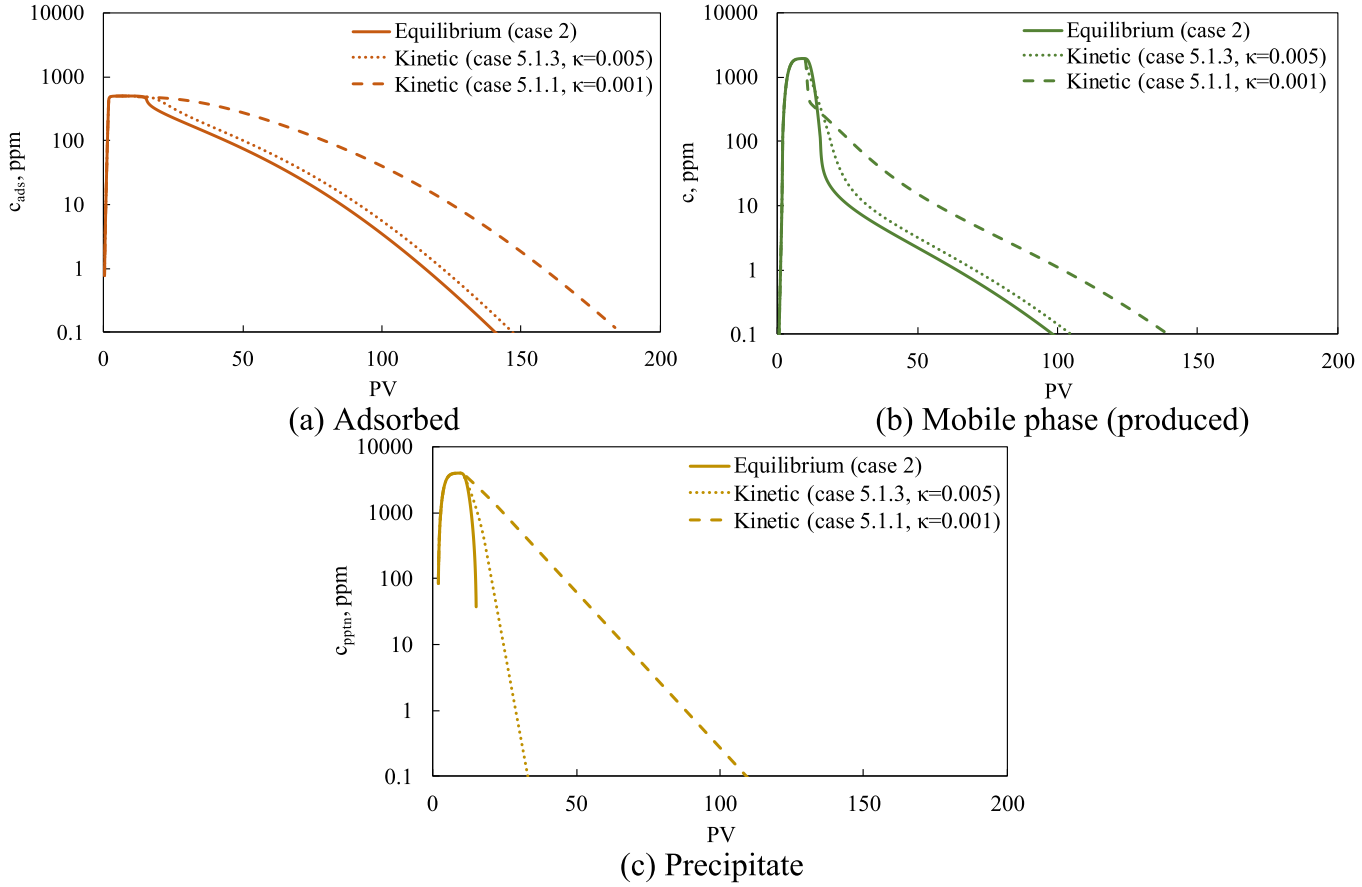

Fig. 12. Effect of k on the concentration profiles of coupled Γ/Π system (outlet cell): a) adsorption, b) solution, c) precipitation.

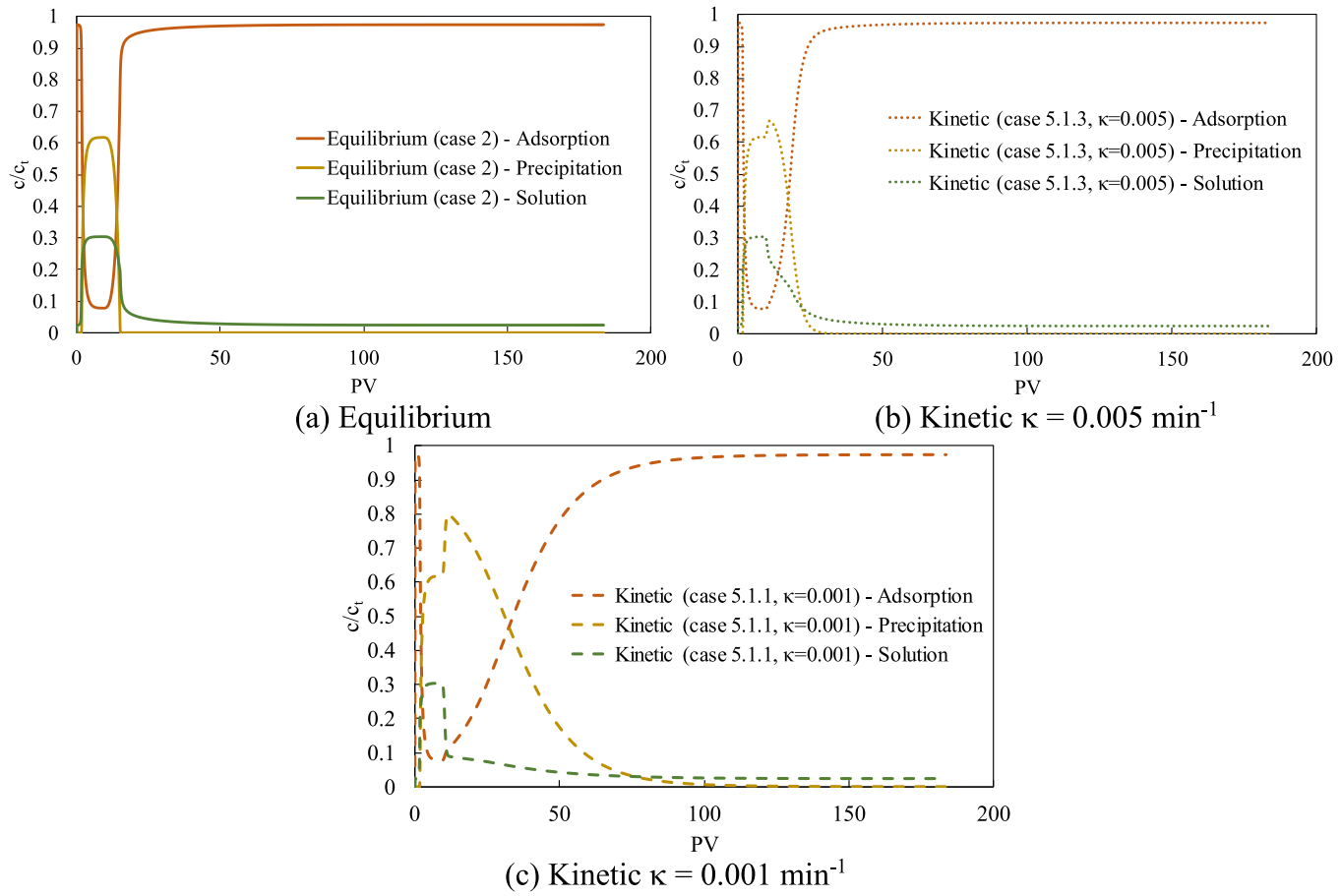

Fig. 13. Effect of κ on the distribution of phases in the coupled Γ/Π system.

Case 5–2: Effect of Γ_{max}

The maximum adsorbed SI level, Γ_{max} (a_2 in the coupled isotherm), is an important parameter that strongly affects the SI adsorption squeeze lifetimes. 4 values of Γ_{max} is considered in Cases 5.2.1 to 5.2.12, as follows; Γ_{max} = 0.05, 0.1, 0.5 and 1 mg/g. Each of these cases is presented for cases of purely adsorption (no precipitation), equilibrium precipitation/adsorption, and kinetic precipitation (dissolution)/adsorption, giving the 12 cases in Table 3, Cases 5.2.1. to 5.2.12.

In this study, the Langmuir isotherm is used which has the form of $\Gamma(c) = \frac{a_1.a_2 c}{(1+a_1 c)}$ where $a_2 = \Gamma_{max}$ and the a_1 parameter (a_1 = K in the common form of Langmuir) defines the shape of the isotherm. Previous theory has established that, at a threshold concentration, c_{th} (usually close to the MIC concentration, and typically ~1–20 mg/L) the length of the SI return effluent to where $c = c_{th}$, is given in terms of postflush PV by a "retardation factor", R_f which depends on the derivative of the isotherm, $(d\Gamma(c)/dc)_{c_t}$ [28,29], where;

$$R_f = \left(1 + \alpha_1 \left(\frac{d\Gamma(c)}{dc}\right)\right) = \left(1 + \frac{\rho}{\phi}\left(\frac{d\Gamma(c)}{dc}\right)\right) \quad (18)$$

For the Langmuir isotherm above, it can be seen that the derivative is given by: $\left(\frac{d\Gamma(c)}{dc}\right) = \frac{a_1.a_2}{(1+a_1 c)^2}$ which, as c becomes very small (near threshold values) it is limited to $\left(\frac{d\Gamma(c)}{dc}\right) \approx a_1.a_2 = K.\Gamma_{max}$. The retardation close to c =0 is therefore approximately $R_f = \left(1 + \frac{\rho a_1 a_2}{\phi}\right) = \left(1 + \frac{\rho K \Gamma_{max}}{\phi}\right)$. Thus, before presenting any calculations of the return effluents, it is clearly expected that the return curve to a threshold (MIC) value of SI concentration c_{th} to be *increased* if Γ_{max} increases in value. The question to be addressed is: will the contribution of the increased Γ_{max} to the squeeze lifetime dominate over the contribution of the kinetic dissolution of the precipitate?

Fig. 14 shows 4 cases of the kinetic, equilibrium, and no precipitation SI return effluents for Γ_{max} = 0.05, 0.1, 0.5, and 1.0 mg/g; which are corresponding to Case 5.2.1 to Case 5.2.12 (Table 3). The main observation here is that as the level of SI adsorption (Γ_{max}) increases, the effect of kinetic precipitation on the longer tail of the SI return reduces quite significantly. For example, in the result in Fig. 14(d) then very little effect of the kinetic precipitation is evident beyond the first ~30PV of the return curve. This may be sufficient or desirable in some cases where a high MIC is required for a relatively short period of the SI return curve. Conversely, if the SI adsorption level is low, then the effect of the kinetic precipitation can be much more significant. As noted above, equilibrium precipitation/dissolution offers very little benefit in any case for the longer-term SI return curve.

To emphasize where the kinetic precipitation can be of some benefit, depending on the MIC value required by the SI, the % increase in lifetime for both the equilibrium and kinetic precipitation (relative to pure adsorption) is shown for 6 MIC values in Fig. 15. The results in Fig. 15 show that the kinetics have a slight effect on the lifetime of the treatment in some cases, for example as shown for Γ_{max}= 1, and MIC<10 ppm, the enhancement is below 2 %. For the cases with low Γ_{max} (e.g. 0.05), as the concentration drops to very low concentrations very quickly, the kinetics are still participating to the SI concentration with a considerable amount related to the solution concentration. In these cases, the kinetics have a higher impact on the enhancement of squeeze lifetime, which can be greater than 30 % (e.g.: Γ_{max}=0.05 mg/g and MIC=10 ppm). As noted above, the conclusion from these results is that the kinetic dissolution is more efficient in lifetime enhancement for lower Γ_{max} and

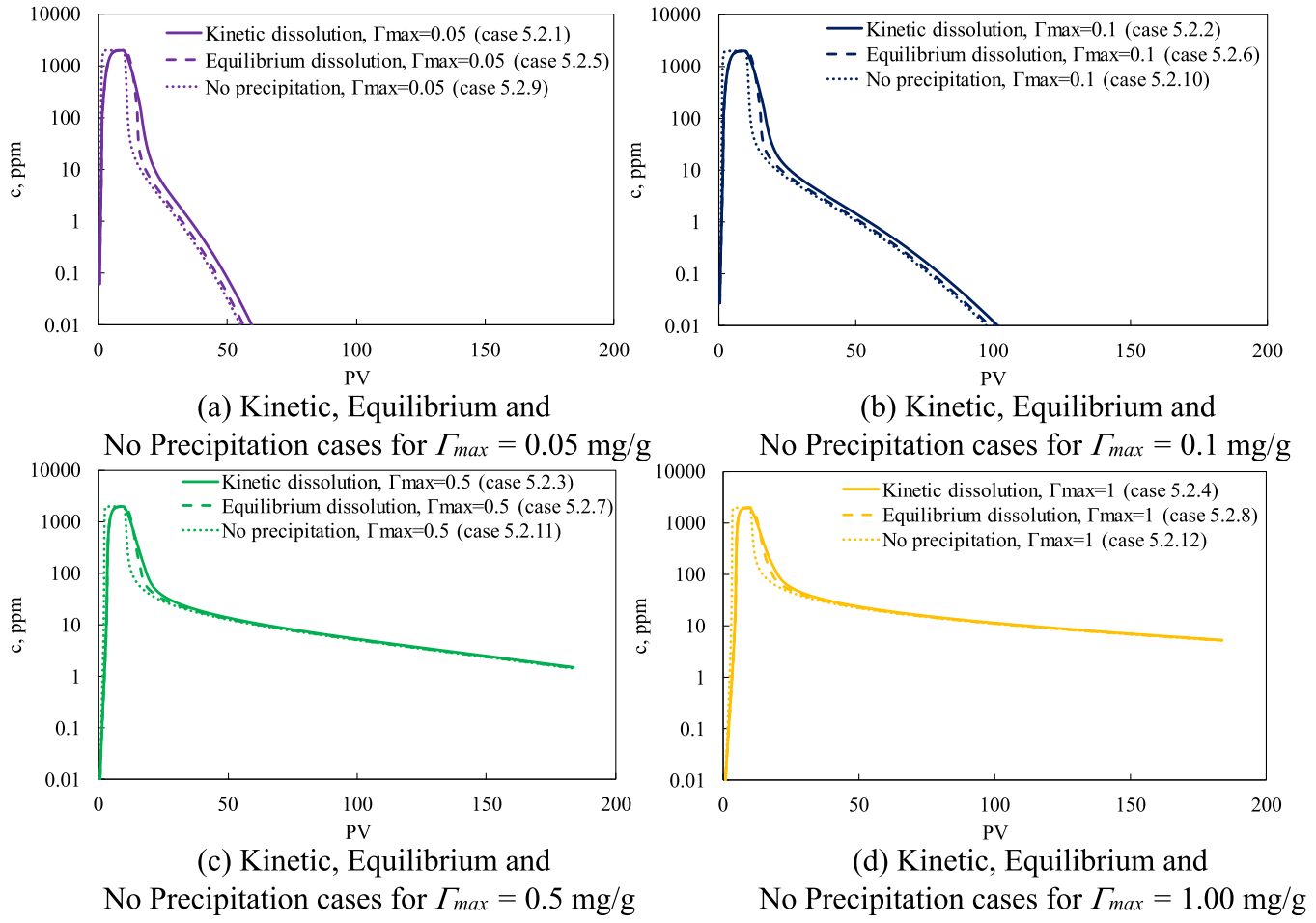

Fig. 14. Effect of Γ_{max} on the return profile of coupled Γ/Π systems and pure adsorption system.

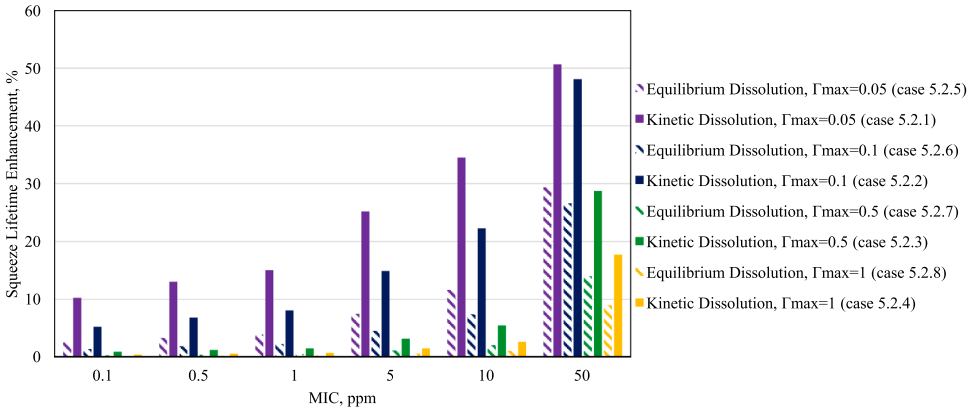

Fig. 15. Effect of Γ_{max} on the performance (squeeze lifetime enhancement) of different systems.

higher MIC values.

Case 5–3: Coupled κ/Γ_{max} Sensitivity

It is clear from calculations above that the effects of the adsorption and kinetic mechanisms on the SI return curves are closely bound together in terms of their impact on the SI squeeze lifetime. For this reason, a combined sensitivity analysis of *both* κ and Γ_{max} is investigated here in Cases 5–3 (Case 5.3.1 to 5.3.9 in Table 3). The transport model was conducted for all combinations of $\kappa = 0.001$, 0.005, and 0.01 min^{-1} and $\Gamma_{max} = 0.05$, 0.10, and 0.5 mg/g. The effect of these combinations on the dimensionless parameters are given in Table 3. The results from these combined κ / Γ_{max} calculations are presented in Fig. 16, where the 3 groups of cases shown are Fig. 16(a) for $\kappa = 0.01$ min^{-1}, Fig. 16(b) for $\kappa = 0.005$ min^{-1} and Fig. 16(c) for $\kappa = 0.001$ min^{-1}, each of which shows results for $\Gamma_{max} = 0.05$, 0.10 and 0.5 mg/g.

The results shown in Fig. 16 confirm several of the previous sensitivities presented above, as expected. In all of the cases shown, the return curve at later times (PV) is very clearly increased for lower SI-precipitate dissolution rates and the mechanism for this has already been described above; i.e. the persistence of the precipitate in "feeding" the flowing phase for a longer period, for the slower the kinetics [or higher flow rates].

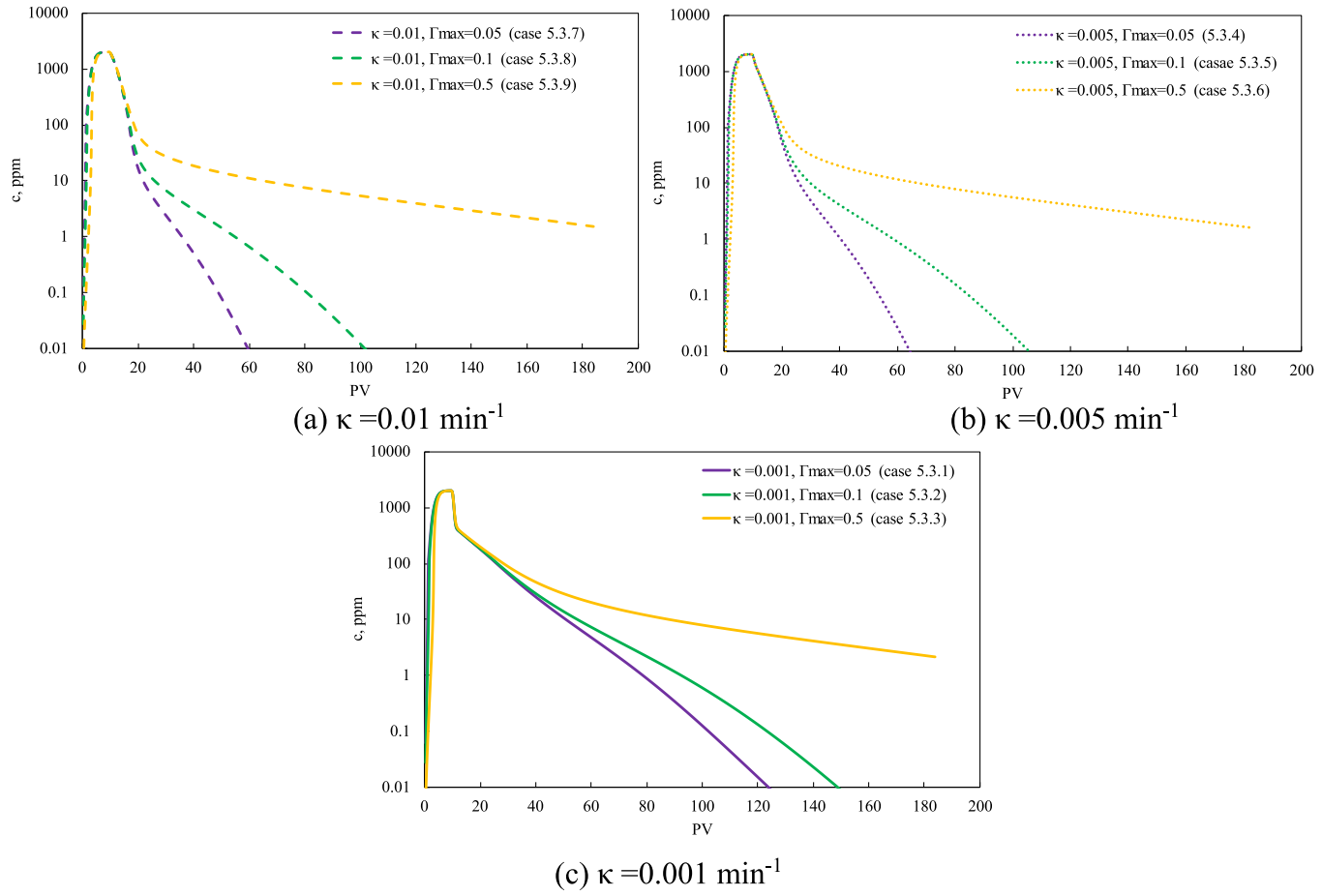

Fig. 16. Effect of combined κ/Γ_{max} on the return profile of coupled Γ/Π systems.

4. Summary and conclusions

In this study, a 1D advection-diffusion-reaction transport model was developed for modeling the scale inhibitor (SI) squeeze treatments in a core flood, including both adsorption and precipitation processes. In this model, a recently developed coupled adsorption/precipitation (Γ/Π) isotherm (demoted $A_{\Pi}(c)$ vs. c) was used to implement the adsorption and precipitation processes in these treatments. Equilibrium adsorption was assumed and modelled using a Langmuir isotherm and both equilibrium and kinetic dissolution of precipitates were considered in the simulations. This model was then used to investigate coupled adsorption/precipitation (Γ/Π) processes in a SI core flood. Since the behavior of pure SI adsorption (both equilibrium and kinetic) is well known and has been explained many times in the literature, this study focused on the conclusion resulting from both equilibrium and (especially) kinetic dissolution effects. These conclusions are related to the "SI squeeze lifetime"; i.e. the time for the extended SI tail in the effluent to reach a certain threshold concentration, c_{th}, which crosses the Minimum Inhibitor Concentration (MIC) level for effective scale inhibition.

The main technical conclusions of this study are as follows:

(i) The precipitation (Π) process can enhance the SI squeeze lifetime working in conjunction with adsorption, which is described by the SI adsorption isotherm, Γ(c). The combined adsorption/precipitation (Γ/Π) process is described by the Γ/Π isotherm, which is denoted, $A_{\Gamma\Pi}(c)$. However, this SI squeeze lifetime extension is very limited for equilibrium precipitation (dissolution) and is only of a significant extent when the dissolution of the precipitate is kinetic, such that the system has a low Damköhler number (N_{Da}). This is achieved by high flow rates (q) or by having very low precipitate dissolution rates (low κ).

(ii) Significant increases in the SI squeeze lifetimes can be achieved at low dissolution rates, but the magnitude of the relative increase in squeeze lifetime is most significant when the level of SI adsorption is lower (i.e. lower Γ_{max}). For higher adsorption cases (i.e. higher Γ_{max}), the SI return curve in the tail can already be sufficiently high, such that the additional benefit of the kinetic precipitation is quite small.

(iii) In cases where some benefit can be achieved, the mechanism of the improved SI return curve is that the slow kinetics of dissolution "feeds" the mobile phase concentration at a value that holds the (equilibrium) isotherm at a steady high value (close to Γ_{max}) for as long as the precipitate is still present. When the precipitate disappears (it is fully dissolved), this feeding effect stops, and from that point, the process is then controlled solely by the adsorption isotherm, $\Gamma(c)$, and the remainder of the flood is determined by this function.

Declaration of Competing Interest

The authors declare that they have no known competing financial interests or personal relationships that could have appeared to influence the work reported in this paper

Data availability

Data will be made available on request.

Acknowledgments

The authors would like to thank the following for sponsorship of the Flow Assurance and Scale Team (FAST) at Heriot-Watt University: Baker Hughes, ChampionX, ChemiServis, Chevron, Clariant, Equinor, Halliburton, Petrobras, Repsol, Shell, SLB, TotalEnergies, Vendanta, Wintershall dea, and Y-tec. Energi Simulation is thanked for funding the Chair in CCUS and Reactive Flow Simulation held by Eric Mackay.

Heriot-Watt University is also thanked for its support through the James-Watt Scholarship programme.

References

[1] O. Vazquez, I. Fursov, E.J. Mackay, Automatic optimization of oilfield scale inhibitor squeeze treatment designs, J. Pet. Sci. Eng. 147 (2016) 302–307, https://doi.org/10.1016/j.petrol.2016.06.025.

[2] M. Kalantari Meybodi, K. Sorbie, O. Vazquez, K. Jarrahian, E. Mackay, A Coupled Model of Phosphonate Scale Inhibitor Interactions with Carbonate Formations, SPE International Conference on Oilfield Chemistry (2023). https://doi.org/10.2118/213819-ms.

[3] O. Vazquez, I. Fursov, E. Mackay, Automatic optimization of oilfield scale inhibitor squeeze treatment designs, J. Pet. Sci. Eng. 147 (2016) 302–307, https://doi.org/10.1016/j.petrol.2016.06.025.

[4] A.T. Kan, Z. Dai, M.B. Tomson, The state of the art in scale inhibitor squeeze treatment, Pet. Sci. (2020), https://doi.org/10.1007/s12182-020-00497-z.

[5] P. Zhang, G. Ruan, D. Shen, A.T. Kan, M.B. Tomson, Transport and return of an oilfield scale inhibitor reverse micelle nanofluid: Impact of preflush and overflush, RSC Adv. 6 (2016) 66672–66681, https://doi.org/10.1039/c6ra07445f.

[6] J. Fink, Scale inhibitors. Petroleum Engineer's Guide to Oil Field Chemicals and Fluids, Elsevier, 2021, pp. 351–391, https://doi.org/10.1016/b978-0-323-85438-2.00007-4.

[7] B. Tomson, A.T. Kan, J.E. Oddo, Acid/base and metal complex solution chemistry of the polyphosphonate DTPMP versus temperature and ionic strength, Langmuir 10 (1994) 1442–1449, https://doi.org/10.1021/la00017a021.

[8] A. Valiakhmetova, K.S. Sorbie, L.S. Boak, S.S. Shaw, Solubility and inhibition efficiency of Phosphonate scale inhibitor-calcium-magnesium complexes for application in a precipitation-squeeze treatment, SPE Prod. Oper. 32 (2017) 343–350, https://doi.org/10.2118/178977-pa.

[9] S.S. Shaw, K.S. Sorbie, Structure, stoichiometry, and modeling of calcium phosphonate scale-inhibitor complexes for application in precipitation-squeeze processes, SPE Prod. Oper. 29 (2014) 139–151, https://doi.org/10.2118/164051-PA.

[10] A.T. Kan, G.M. Fu, M.B. Tomson, M. Al-Thubaiti, A.J. Xiao, Factors affecting scale inhibitor retention in carbonate-rich formation during squeeze treatment, Spe J. 9 (2004) 280–289, https://doi.org/10.2118/80230-PA.

[11] M. Kalantari Meybodi, K.S. Sorbie, O. Vazquez, E.J. Mackay, K. Jarrahian, M. Igder, A comprehensive equilibrium model for the phosphonate scale inhibitor-carbonate system including coupled adsorption/precipitation (G/P), Colloids Surf. A: Physiochem. Eng. Asp. (2024) 133535, https://doi.org/10.1016/j.colsurfa.2024.133535.

[12] O. Vazquez, V. Azari, I. Fursov, E. Igben, E. Mackay, Uncertainty quantification of pseudo-adsorption isotherm history matching, SPE International Oilfield Scale Conference and Exhibition (2020). https://doi.org/10.2118/200715-ms.

[13] E.J. Mackay, M.M. Jordan, Squeeze Modelling: Treatment Design and Case Histories, 5Th Spe Europe Formation Damage Conference (2003). https://doi.org/10.2118/82227-MS.

[14] V. Azari, O. Vazquez, E. Mackay, K. Sorbie, M. Jordan, Gradient descent algorithm to optimize the offshore scale squeeze treatments, J. Pet. Sci. Eng. 208 (2022), https://doi.org/10.1016/j.petrol.2021.109469.

[15] N.M. Farooqui, K.S. Sorbie, The use of PPCA in scale-inhibitor precipitation squeezes: solubility, inhibition efficiency, and molecular-weight effects, SPE Prod. Oper. 31 (2016) 258–269, https://doi.org/10.2118/169792-PA.

[16] E. Mackay, M.M. Jordan, SQUEEZE Modelling: Treatment Design and Case Histories, SPE European Formation Damage Conference (2003). https://doi.org/10.2118/82227-MS.

[17] M.M. Jordan, K. Sjuraether, G. Seland, H. Gilje, The use of scale inhibitor squeeze placement software to extend squeeze life and reduce operating costs in mature high temperature oilfields, NACE - Int. Corros. Conf. Ser. (2000).

[18] B. Ghosh, X. Li, Effect of surfactant composition on reservoir wettability and scale inhibitor squeeze lifetime in oil wet carbonate reservoir, J. Pet. Sci. Eng. 108 (2013) 250–258, https://doi.org/10.1016/j.petrol.2013.04.012.

[19] M.M. Jordan, E.J. Mackay, O. Vazquez, The Influence of Overflush Fluid Type on Scale Squeeze Life Time – Field Examples and Placement Simulation Evaluation, Corrosion (2008).

[20] A.T. Kan, G.M. Fu, M.B. Tomson, M. Al-Thubaiti, A.J. Xiao, Factors affecting scale inhibitor retention in carbonate-rich formation during squeeze treatment, Spe J. 9 (2004) 280–289, https://doi.org/10.2118/80230-PA.

[21] K. Jarrahian, K. Sorbie, M. Singleton, L. Boak, A. Graham, Building a fundamental understanding of scale-inhibitor retention in carbonate formations, SPE Prod. Oper. 35 (2020) 85–97, https://doi.org/10.2118/193635-MS.

[22] M. Kahrwad, K.S. Sorbie, L.S. Boak, Coupled adsorption/precipitation of scale inhibitors: Experimental results and modeling, SPE Prod. Oper. 24 (2009) 481–491, https://doi.org/10.2118/114108-PA.

[23] M.M. Jordan, K.S. Sorbie, P. Griffint, S. Hennessey, K.E. Hourston, P. Waterhouse, Scale Inhibitor Adsorption/Desorption vs. Precipitation: The Potential for Extending Squeeze Life While Minimising Formation Damage, SPE European Formation Damage Conference (1995). https://doi.org/10.2118/30106-MS.

[24] J. Ibrahim, K.S. Sorbie, L.S. Boak, Coupled Adsorption/Precipitation Experiments: 1. Static Results, SPE International Conference and Exhibition on Oilfield Scale (2012) 281–303. https://doi.org/10.2118/155109-MS.

[25] F. Yan, F. Zhang, N. Bhandari, L. Wang, Z. Dai, Z. Zhang, Y. Liu, G. Ruan, A. Kan, M. Tomson, Adsorption and precipitation of scale inhibitors on shale formations, J. Pet. Sci. Eng. 136 (2015) 32–40, https://doi.org/10.1016/j.petrol.2015.11.001.

[26] K. Jarrahian, L. Boak, A. Graham, M. Singleton, K. Sorbie, Experimental Investigation of the interaction between a phosphate ester scale inhibitor and carbonate rocks for application in squeeze treatments, Energy Fuels 33 (2019) 4089–4103, https://doi.org/10.1021/acs.energyfuels.9b00382.

[27] W.S. Thomas, K.S. Sorbie, M.A. Singleton, Coupled Adsorption/Precipitation Tests with a Phosphonate Inhibitor and Carbonate Substrate, SPE International Oilfield Scale Conference (2014). https://doi.org/10.2118/SPE-169779-MS.

[28] K.S. Sorbie, A General Coupled Kinetic Adsorption/Precipitation Transport Model for Scale Inhibitor Retention in Porous Media: I. Model Formulation, SPE International Conference on Oilfield Scale (2010). https://doi.org/10.2118/130702-MS.

[29] A. Stamatiou, K.S. Sorbie, Analytical solutions for a 1D scale inhibitor transport model with coupled adsorption and precipitation, Transp. Porous Media 132 (2020) 591–625, https://doi.org/10.1007/s11242-020-01405-0.

[30] O. Vazquez, K.S. Sorbie, E.J. Mackay, A General Coupled Kinetic Adsorption/Precipitation Transport Model for Scale Inhibitor Retention in Porous Media: II. Sensitivity Calculations and Field Predictions, SPE International Conference on Oilfield Scale (2010). https://doi.org/10.2118/130703-MS.

[31] M.Dong Yuan, K. Sorbie, A. Todd, L. Atkinson, The Modelling of Adsorption and Precipitation Scale Inhibitor Squeeze Treatments in North Sea Fields SPE Members. SPE International Symposium on Oilfield Chemistry, 1993, https://doi.org/10.2118/25163-MS.

[32] M. Kahrwad, K.S. Sorbie, L.S. Boak, Coupled adsorption/precipitation of scale inhibitors: experimental results and modeling, SPE Prod. Oper. 24 (2009) 481–491, https://doi.org/10.2118/114108-PA.

[33] O. Vazquez, P. Thanasutives, C. Eliasson, N. Fleming, E. Mackay, Modeling the application of scale-inhibitor-squeeze-retention-enhancing additives, SPE Prod. Oper. 26 (2011) 270–277, https://doi.org/10.2118/141384-PA.

[34] S. Baraka-Lokmane, K.S. Sorbie, Scale Inhibitor Core Floods in Carbonate Cores: Chemical Interactions and Modelling. SPE Eighth International Symposium on Oilfield Scale, 2006, pp. 210–223, https://doi.org/10.2118/100515-MS.

[35] K.S. Sorbie, P. Jiang, M.D. Yuan, P. Chen, M.M. Jordan, a C. Todd, The Effect of pH, Calcium, and Temperature on the Adsorption of Phosphonate Inhibitor Onto Consolidated and Crushed Sandstone, SPE Annual Technical Conference and Exhibition (1993), https://doi.org/10.2118/26605-MS.

[36] O. Vazquez, E. Mackay, K. Sorbie, A two-phase near-wellbore simulator to model non-aqueous scale inhibitor squeeze treatments, J. Pet. Sci. Eng. 82–83 (2012) 90–99, https://doi.org/10.1016/j.petrol.2011.12.030.

[37] J. Ibrahim, K.S. Sorbie, L.S. Boak, Coupled Adsorption/Precipitation Experiments: 1. Static Results. SPE International Conference and Exhibition on Oilfield Scale, 2012, pp. 281–303, https://doi.org/10.2118/155109-MS.

[38] A. Malandrino, E. Spa, M.D. Yuan, K.S. Sorbie, M.M. Jordan, Mechanistic Study and Modelling of Precipitation Scale Inhibitor Squeeze Processes. SPE International Symposium on Oilfield Chemistry, 1995, https://doi.org/10.2118/29001-MS.

[39] F. Yan, F. Zhang, N. Bhandari, L. Wang, Z. Dai, Z. Zhang, Y. Liu, G. Ruan, A. Kan, M. Tomson, Adsorption and precipitation of scale inhibitors on shale formations, J. Pet. Sci. Eng. 136 (2015) 32–40, https://doi.org/10.1016/j.petrol.2015.11.001.

[40] A.T. Kan, Z. Dai, M.B. Tomson, The state of the art in scale inhibitor squeeze treatment, Pet. Sci. (2020), https://doi.org/10.1007/s12182-020-00497-z.

[41] K.S. Sorbie, A Simple Model of Precipitation Squeeze Treatments, SPE International Conference on Oilfield Scale (2012). https://doi.org/10.2118/155111-MS.

[42] K. Jarrahian, K. Sorbie, M. Singleton, L. Boak, A. Graham, The effect of pH and mineralogy on the retention of polymeric scale inhibitors on carbonate rocks for application in squeeze treatments, SPE Prod. Oper. 34 (2019) 344–360, https://doi.org/10.2118/189519-PA.

[43] K.S. Sorbie, A. Stamatiou, Analytical solutions of a one-dimensional linear model describing scale inhibitor precipitation treatments, Transp. Porous Media 123 (2018) 271–287, https://doi.org/10.1007/s11242-018-1040-3.